Step-index High Absorption Yb-doped Large-mode-area Fiber with Ge-doped Raised Cladding

Raghuraman Sidharthan,[1] Junhua Ji,[2] Kang Jie Lim,[3] Serene Huiting Lim,[3] Huizi Li,[1] Jian Wei Lua,[1] Yanyan Zhou,[1] Chun Ho Tse,[1] Daryl Ho,[1] Yue Men Seng,[1] Song Liang Chua,[3] and Seongwoo Yoo[1,*]

[1] School of Electrical and Electronic Engineering, Centre of Optical Fiber Technology, The Photonics Institute, Nanyang Technological University, 50 Nanyang Avenue, 639798, Singapore

[2] KLA-Tencor Pte. Ltd., 4 Serangoon North Ave 5, 554532, Singapore

[2]DSO National Laboratories, Singapore

*Corresponding author: seon.yoo@ntu.edu.sg

Received XX Month XXXX; revised XX Month, XXXX; accepted XX Month XXXX; posted XX Month XXXX (Doc. ID XXXXX); published XX Month XXXX

We report an all-solid large mode area (LMA) step-index fiber offering high absorption and low core numerical aperture (NA) by introducing highly Ytterbium-doped P:Al core and Germanium-doped cladding. The fiber provides core absorption of ~1200 dB/m at 976 nm with a low 0.07 core NA thanks to the raised Ge cladding. Furthermore, matched profiles of P and Al across core is successfully obtained with high concentration of Yb_2O_3 above 0.4 mol%. The fiber characteristics are routinely achievable by the conventional modified chemical vapor deposition with a solution doping technique. Highly efficient laser with >100 W output power, 86% slope efficiency with respect to launched pump power and a mean M^2 of 1.34 has been demonstrated using the fabricated LMA step-index fiber. We also report 80% laser slope efficiency with 58 W output power (pump power limited) within only 0.5 m of the fiber when pumped by a wavelength-stabilized laser diode.

OCIS codes: *(060.2280) Fiber design and fabrication; (060.2300) Fiber measurements; (140.3615) Lasers, ytterbium*

The advances in performance of Ytterbium-doped fiber (YDF) lasers have been remarkable in the past couple of decades, making them a choice of variety of industrial applications. Excellent power conversion efficiency, high power stability and superior beam quality are a few of the unique features of YDF lasers that differentiate it from other solid state lasers especially for high power applications. However, lower nonlinear thresholds leaves it at a disadvantage for applications requiring high peak powers, high pulse energies or narrow linewidth [1]. Using a highly Yb-doped, shorter piece of fiber with a large effective mode area is the way to mitigate the issue of lower nonlinear thresholds. However, higher Yb doping leads to higher numerical aperture (NA), thus yielding poor beam quality. The high Yb concentration also increases the chances of clustering related problems such as photodarkening (PD).

Alternatively, the short absorption length can be attained by introducing a low cladding-to-core area ratio (CCAR) instead of higher Yb concentration. This approach can separate the low core NA requirement from the high absorption requirement, and becomes the dominant design route to satisfy high absorption and low core NA simultaneously. However, the low CCAR is challenging to obtain in a step-index fiber with low core NA due to arising of micro-bending loss [2]. Thus, micro-structured fibers with an air cladding layer have been the fiber of choice for applications requiring a short absorption length fiber. For example, a rod type fiber was reported to provide pump absorption of 30 dB/m at 976 nm in a CCAR of 12.25 with an index matched core [3]. Its corresponding core absorption is ~368 dB/m. Also, a micro-structured fiber with a pump absorption of 10 dB/m in a CCAR of 25 is commercially available [4]. Its corresponding core absorption is ~250 dB/m. In contrast, an all-solid LMA step-index fiber with a 20 μm core size and 0.06 core NA typically offers 1 dB/m pump absorption with a CCAR of 400, which corresponds to 400 dB/m core absorption. This core absorption is slightly higher than the micro-structured fiber counterparts. Apparently, this comparison witnesses a unique advantage of the micro-structured fibers, say high absorption without demanding high Yb concentration, permitting short absorption length which is essential to suppress nonlinearities. However, handling is a persisting issue with the micro-structured fibers. Splicing, cleaving and connectivity to other fibers or fiber components are not straightforward. An all-solid LMA fiber stands out in this aspect, not to mention its cost-effective fabrication route. Perhaps the most promising approach so far to the high absorption step index LMA fiber is to adopt a pedestal layer around a highly Yb-doped core [5-7]. The pedestal layer effectively lowers the core NA. However, the size of the pedestal has to be chosen carefully. Deviation from the optimum size can affect the mode field diameter, or may couple out core modes to the pedestal or may trap pump light in a helical trajectory in the pedestal [7]. The trapped pump beam is wasted because the pedestal cannot be shaped to increase overlap with Yb ions. In order to overcome such limitations, all glass double clad structure with raised cladding has been reported [8]. In the reported work, the fiber with Yb:Al core and Ge-doped inner cladding has been fabricated using outside vapor deposition technique. Yb concentration of 1.2 wt% was reported in a 30/350 μm fiber with a low core NA of <0.05.

However, as both Yb and Al dopants increase the core index, it requires high doping levels of germanium in the inner cladding to lower the core NA. Increasing Ge would induce fabrication complexity due to, for example, high vapor pressure of GeO_2. Moreover, the high Yb concentration in aluminosilicate core is subject to photodarkening [9].

Another approach to reduce the core NA is to co-dope Phosphorous (P) and Aluminum (Al) [10-14]. When Al and P coexist at an equivalent molar ratio, they form $AlPO_4$ that mimics SiO_2 structure and obtain the same refractive index of silica. The presence of P greatly suppresses photodarkening as well, which is an additional advantage. A great deal of effort has been made towards achieving such Yb/Al/P co-doped core. However, previous reports seem to suggest that achieving highly Yb doped Al:P composition is very challenging in aspects of index profile control and low background loss. Evaporation of Yb or P [12, 13], or non-uniform distribution of the dopants [10, 14] causes index profile distortion in the core. We have recently reported fabrication of a highly Yb-doped (0.5 mol% Yb_2O_3, equivalent to ~3 wt% Yb), step-index Al:P equi-molar fiber with very good index control, using the conventional modified chemical vapor deposition (MCVD) and solution doping technique [15]. Although the expected index suppression was observed, the core NA was higher (~0.1) than a conventional LMA fiber because of the high Yb concentration. Hence, to achieve lower NA and high concentration, this approach alone is not sufficient.

In this work, we report a step-index LMA high absorption fiber. Fabrication of highly Yb doped Al:P core with Ge cladding is presented. The fiber provides ~ 1200 dB/m core absorption at 976 nm and its core NA is controlled below 0.07 by the raised Ge-doped cladding. It's CCAR of the Ge cladding and Yb core is 54, hence leading to 22 dB/m cladding absorption which is twice of the micro-structured fibers. Furthermore, we demonstrate uniformly matched P: Al core composition to accommodate the high Yb concentration and for PD suppression. We have successfully achieved >100 W output power with M^2 of ~1.34 at 86% slope efficiency using the fabricated fiber. We have also achieved ~80% slope efficiency with respect to launched power in only 0.5 m of the fabricated fiber under wavelength-stabilized laser diode pumping, evidencing drastically reduced absorption length in a step-index LMA laser fiber.

Fiber preform fabrication constituted of mainly three stages including Ge-doped cladding deposition, high Yb doped P: Al core deposition, and silica outer cladding removal and octagonal shaping. The raised cladding was realized by depositing multiple layers of GeO_2-SiO_2 by flowing in gas mixture of $SiCl_4$ and $GeCl_4$ into the silica substrate tube. Since the tube undergoes gradual collapsing over the depositions due to high temperature from a H_2/O_2 burner, a backward pressurizing system was employed to keep the tube open. During the deposition, the burner temperature and the gas flow rates were adjusted to compensate additional temperature gradient, thus maintaining same thermophoresis force over the depositions [16]. With the developed recipe, we can routinely achieve raised Ge cladding of 6 - 9 mm thickness and a raised index contrast of 0.015 – 0.020 from silica. The doped Ge content is estimated in the range of ~12 mol% of GeO_2 [17]. Thus, the superior physical and chemical properties of silica are not compromised. We have not noticed abnormality while splicing and cleaving this fiber although more systematic study is required to confirm its characteristics. The Ge cladding deposition is followed by a core deposition of Yb:Al:P doped silica. We use phosphosilicate soot and a solution doping technique to introduce Yb and Al. A uniform and stable P_2O_5–SiO_2 soot is deposited using the MCVD reagents of $SiCl_4$ and $POCl_3$. A pre-sintering pass was employed to stabilize the deposited P_2O_5–SiO_2 soot and control its porosity [11]. Later Yb and Al were introduced via the solution doping technique [14]. Subsequently, the conventional preform fabrication steps were carried out to sinter the soot, collapse the tube and seal it to a preform. We intentionally feed in extra $POCl_3$ flow during the high temperature collapse passes to compensate for the evaporation of P due to its high vapor pressure. The fabricated preform with triple layers of core, Ge cladding and silica cladding was later milled down to the Ge doped cladding layer, thus completely removing the outer silica layer from the preform rod. While removing the silica cladding, the preform was shaped to an octagonal cross-section under the milling to improve pump absorption. The milled preform was later polished and drawn in low index acrylic coating to form a double clad laser fiber.

A microscopic image of a representative fiber of the Al:P:Yb core and the Ge cladding is shown in Fig. 1 (a). Its core diameter is measured to be 19 µm and cladding (flat to flat) diameter of 136 µm. Its CCAR is then calculated to be ~54, offering at least twice of the micro-structured fibers. The index profile of the fiber was measured using an IFA 100 index profiler and is shown in Fig. 1(b). It should be noted that the baseline accounts for index matching oil rather than silica. The fiber is silica cladding-less. Nonetheless, the index difference between the index matching oil and the Ge cladding well represents raised index of the Ge cladding with respect to the silica. It measures 0.0018 with ±0.0004 transverse tolerance. In addition, the deposited Ge cladding exhibits a flat and uniform index profile, which is important to serve as a cladding with no extra influence to a guiding property. The index difference between the core and the Ge-doped cladding was found to be 0.0017 with a slight index dip of ±0.0004. This corresponds to a core NA of ~0.07. We note that the core NA is adjustable in our fabrication by controlling the index level of Ge cladding.

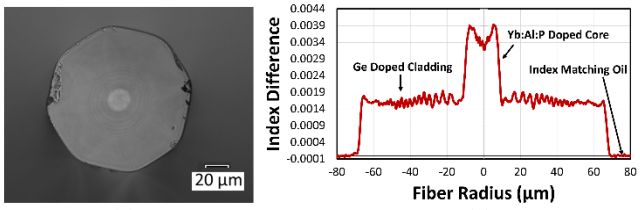

(a) (b)

Fig. 1. (a) Microscopic image of the fiber end facet and (b) Index profile of the fabricated double clad fiber with Yb:Al:P doped core and Ge-doped inner cladding.

Fig. 2 (a) shows the concentration profile of dopants measured using Energy Dispersive X-ray Spectroscopy (EDX) across a representative fiber core. Peak concentrations of Yb_2O_3, Al_2O_3 and P_2O_5 in the fiber core were found to be ~0.4 mol%, ~4.4 mol% and ~4.8 mol%, respectively. Apparently, flap top profiles were achieved in all the dopants. In particular, absence of central dip in P_2O_5 distribution across core shows that our fabrication process well compensated the high vapor pressure of P_2O_5 during the MCVD run. We intentionally raised the P_2O_5 slightly higher than Al_2O_3 to

suppress PD further. More interestingly, the combined nearly 10 mol% of refractive index raising elements only increases the index contrast by ~0.0035 from silica. This clearly demonstrates index suppression by forming $AlPO_4$ otherwise leading to 0.014 index increase by Al:Yb or 0.0085 by P:Yb only core. We note that the intentionally higher P over Al concentration resulted in slightly higher index than a perfect 1:1 ratio of P:Al. However, this is not a concern for us because the raised index can be compensated by the raised Ge-doped cladding. Consequently, the actual core index contrast becomes 0.0017 with respect to the cladding. Consequently, our fabrication allows the desired characteristics of high concentration, low PD and low core NA, manifesting itself as a unique LMA step-index fiber. Cladding absorption in the fiber was later measured using a cutback method employing a white light source and an optical spectrum analyzer (OSA). The measured absorption is shown in Fig. 2 (b). Cladding absorption values of ~8 dB/m and 22.3 dB/m was observed at 915nm and 976nm respectively.

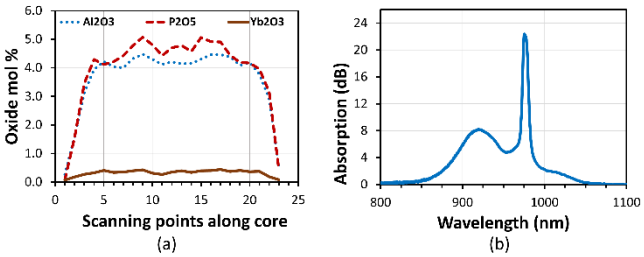

Fig. 2. (a) Dopant concentration in oxide mol% measured using EDX and (b) Fiber cladding absorption measurement.

The high cladding absorption of 22.3 dB/m at 976 nm is mainly attributed to the high concentration of Yb. More importantly, the cladding absorption is translated to 1205 dB/m of core absorption with the fiber CCAR of 54. This core absorption in conjunction with the core NA of 0.07 well represents a potential for a high power ultrafast pulsed laser fiber as an alternative to the micro-structured fibers.

The absorption and emission cross-sections of the fabricated fiber is shown in Fig. 3(a) and is seen to be quite similar to that reported in other similar works with Yb, Al and P doped core [14]. A PD level in the fiber was examined in a core pumping configuration as detailed in [18]. A wavelength of 634 nm is selected as probe light since the PD induced loss can be easily detected and the wavelength is also located far from the Yb-band. A short piece of fiber of length ~1.5 cm was selected to suppress undesired amplified stimulated emission and keep uniform inversion level through the fiber. A commercial software (FiberPower) was used to calculate the inversion level at launched pump power. A pump power of 120 mW at 975 nm produces 42% inversion along the fiber. The measurement was performed for around 1 hour. The measured temporal decay at 634 nm is represented in Fig. 3 (b) which indicates very low PD loss of ~10 dB/m at 634 nm.

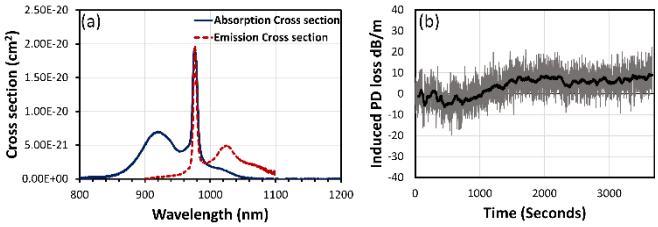

Fig. 3. (a)Absorption and emission cross-sections for the fiber and (b) PD induced temporal excess loss for the fiber at 634 nm under 975 nm pumping.

In order to study laser performance, a fiber was drawn to 19 and 136 μm core and cladding sizes, respectively. The fiber was coated with a low index coating material which provides 0.45 NA with respect to silica glass. We employed a free running 4%-4% linear cavity as shown in Fig. 4. Dichroic mirrors were used to separate the signal and pump beams at both input and output ends. The pump laser was switched between a wavelength unstabilized laser diode (LD) and a wavelength stabilized LD at 975 nm. The laser spectrum, slope efficiency and beam quality were evaluated in this work. Two sets of experiments are reported here: the first using the wavelength unstabilized LD pumping a 2 m long fiber, and the second using a wavelength stabilized LD pumping a 0.5m long fiber. In both cases, the fiber under test has been coiled into loops of 5cm diameter to filter out higher order modes as much as possible. Setting the bending diameter to ~5cm was found to result in near single mode operation. The 2m long fiber was cladding pumped by the unstabilized LD, and it generated 107 W of output power at 1050 nm. The laser signal output power is plotted against the launched pump power as shown by diamond markers in Fig. 5(a). Its laser slope efficiency is measured as ~86%. The laser output spectrum at the full power is shown in the inset (1) of Fig. 5 (a) and was observed to peak at ~1050nm. Note that the pump wavelength shifts from 965 nm to 970 nm in our measurement. The drifting and unmatched wavelength to the Yb peak absorption required the fiber to be long (2 m). Later, the same experiment was repeated using the wavelength stabilized LD. Thanks to the good overlap with the Yb peak absorption wavelength, the fiber length can be shortened to 0.5 m. The laser performance is shown by circular markers in Fig. 5 (a). A maximum output power of 58.6 W was observed at 71.5 W of launched pump power. The output power is only limited by the available pump power. From the plot, the laser slope efficiency is measured to be ~80%. Laser output spectrum at the full power is centered on 1035 nm as shown in the inset (2) in Fig. 5(a). Nonlinearity threshold is proportional to A_{eff}/L where A_{eff} is an effective area, and L denotes fiber length. Considering 10 dB absorption as a required length for efficient laser performance, our fiber offers 20 times higher suppression than a conventional LMA fiber with the same core size. For average power scaling, thermal related issues such as transverse mode instability (TMI) also needs to be tackled. We believe that our step-index fiber allows the conventional mode selective bending scheme to suppress the HOMs, thus the TMI, as demonstrated in, e.g. [19]. The beam quality of the fiber was later evaluated at the maximum output signal power through the M^2 factor. Fig. 5 (b) shows the results of M^2 measurement at ~107 W output power. Reasonably good beam quality with a mean M^2 value of 1.34 was observed for the 0.07 core NA fiber. The M^2 values along x and y directions were found to be

1.29 and 1.39 respectively. The variation along x and y directions can be attributed to the slight ellipticity of the fiber core.

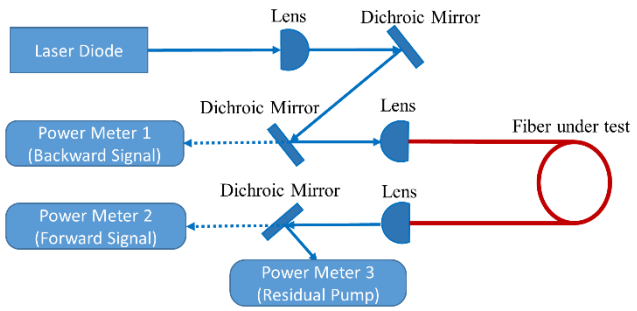

Fig. 4. Fiber laser experimental setup. The solid line arrow indicates pump beam direction, and the dashed line arrow follows signal beams.

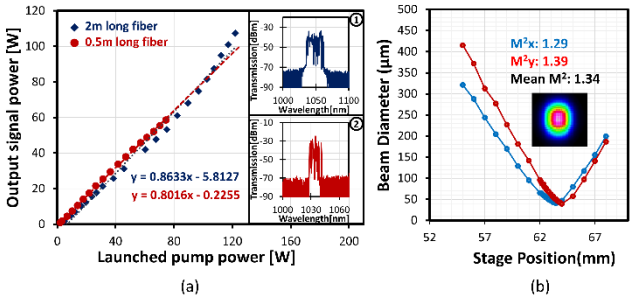

Fig. 5. (a) Laser output power versus pump power in a 2m long fiber pumped using wavelength unlocked diode source and in a 0.5m long fiber pumped using 976nm wavelength locked diode source. The inset (1) shows the laser spectrum at full power in 2 m long fiber and inset (2) shows the laser spectrum at full power in 0.5 m long fiber; (b) measured beam quality factor at 107 W output power in a 2 m long fiber, with an inset showing beam profile.

In conclusion, a high absorption Ge-clad fiber with Yb:Al:P doped core was fabricated by the MCVD and solution doping method. The fabricated fiber offers a very short absorption length and has a core absorption of ~1200 dB/m at 976 nm. Such high absorption in a step index fiber with low NA core shows potential for applications requiring very short absorption lengths. The low core NA was obtained by means of raised Ge-doped cladding as well as P:Al core. The core was co-doped with equi-molar quantities of P and Al to suppress PD and to reduce the core NA. The laser performance using short lengths of the fabricated fiber was evaluated. In one set of experiments, >100 W of output signal power was demonstrated at a slope efficiency of 86% in a 2 m long fiber using a wavelength unstabilized pump source. Later, ~80% slope efficiency was demonstrated in a very short piece of ~0.5 m of fiber using a wavelength locked pump source. The maximum output power of 58.6 W was demonstrated in such short piece of fiber, which was limited only by the available pump power. Here the absorption length has been reduced considerably as compared to other step-index LMA fibers. Such reduced absorption length increases the nonlinearity threshold and can be useful in applications involving high peak powers and high pulse energies. To the best of our knowledge, this is the first report on such high Yb doped equimolar Al:P core cladded by germanosilicate glass.

References

1. M. N. Zervas and C. A. Codemard, IEEE J. Sel. Top. Quantum Electron. **20,** 219-241 (2014).
2. M. E. Fermann, Opt. Lett. **23**, 52-54 (1998).
3. Limpert, O. Schmidt, J. Rothhardt, F. Röser, T. Schreiber, A. Tünnermann, S. Ermeneux, P. Yvernault, and F. Salin, Opt. Express **14**, 2715-2720 (2006).
4. NKT Photonics White Paper, "Modal properties of the DC-200/40-PZ-Yb LMA fiber" (NKT Photonics 2013).
5. P. Laperle, C. Paré, H. Zheng, A. Croteau, Y. Taillon, Proc. SPIE **6343**, 63430X (2006).
6. S. Yoo, A. S. Webb, A. J. Boyland, R. J. Standish, A. Dhar and J. K. Sahu, Laser Phys. Lett. **8**, 453-457(2011).
7. K. Tankala, B. Samson, A. Carter, J. Farroni, D. Machewirth, N. Jacobson, U. Manyam, A. Sanchez, M-Y. Chen, A. Galvanauskas, W. Torruellas, Y. Chen, Proc. SPIE **6102**, 610206 (2006).
8. J. Wang, S. Gray, D. Walton, M. Li, X. Chen, A. Lu, A. Z. Luis, Proc. SPIE, **6890,** 689006 (2008).
9. S. Jetschke, S. Unger, M. Leich, and J. Kirchhof, Appl. Opt. 51, 7758-7764 (2012).
10. S. Jetschke, S. Unger, A. Schwuchow, M. Leich, and J. Kirchhof, Opt. Express **16**, 15540-15545 (2008).
11. K. Ichii, S. Tanjigawa, T. Arai., U.S.Patent USOO8774590B2, (2014).
12. C. Hupel, S. Kuhn, S. Hein, N. Haarlammert, J. Nold, F. Beier, B. Sattler, T. Schreiber, R. Eberhardt, and A. Tünnermann, in *Advanced Solid State Lasers*, OSA Technical Digest (Optical Society of America, 2015), paper AM4A.2
13. C. Gao, Z. Huang, Y. Wang, H. Zhan, L. Ni, K. Peng, Y. Li, Z. Jia, X. Wang, A. You, X. Xiang, J. Wang, F. Jing, H. Lin, and A. Lint, J. Lightwave Technol. **34**, 5170-5174 (2016).
14. S. Unger, A. Schwuchow, S. Jetschke, V. Reichel, M. Leich, A. Scheffel, and J. Kirchhof, Proc. SPIE **7212,** 72121B (2009).
15. R. Sidharthan, S. H. Lim, K. J. Lim, D. Ho, C. H. Tse, J. Ji, H. Li, Y. M. Seng, S. L. Chua, and S. Yoo, in *Conference on Lasers and Electro-Optics*, OSA Technical Digest (Optical Society of America, 2018), paper JTh2A.129.
16. P. G. Simpkins, S. Greenberg-Kosinski, and J. B. MacChesney, J. Appl. Phys. **50**, 5676-5681 (1979).
17. E. M. Dianov and V. M. Mashinsky, J. Lightwave Technol. **23**, 3500-3508 (2005).
18. H. Li, L. Zhang, R. Sidharthan, D. Ho, X. Wu, N. Venkatram, H. Sun, T. Huang, and S. Yoo, J. Lightwave Technol. **35**, 2535-2540 (2017).
19. F. Beier, F. Möller, B. Sattler, J. Nold, A. Liem, C. Hupel, S. Kuhn, S. Hein, N. Haarlammert, T. Schreiber, R. Eberhardt, and A. Tünnermann, Opt. Lett. **43**, 1291-1294 (2018).